

An energy efficient trajectory tracking controller for car-like vehicles using Model Predictive Control

Conference Paper**Author(s):**

Salazar, Mauro; Alessandretti, Andrea; Aguiar, A. Pedro; Jones, Colin N.

Publication date:

2015

Permanent link:

<https://doi.org/10.3929/ethz-a-010575649>

Rights / license:

[In Copyright - Non-Commercial Use Permitted](#)

Originally published in:

<https://doi.org/10.1109/CDC.2015.7402789>

An Energy Efficient Trajectory Tracking Controller for Car-like Vehicles using Model Predictive Control

Mauro Salazar^{1,2}, Andrea Alessandretti^{2,3}, A. Pedro Aguiar⁴ and Colin N. Jones²

Abstract—A Model Predictive Control (MPC) strategy for energy efficient motion control of car-like vehicles is presented. First, a nonlinear control law for trajectory tracking is derived and used to design a trajectory tracking MPC controller with convergence guarantees to a desired position trajectory. Then, assuming electric propulsion, a performance index reflecting the energy consumption of the vehicle is derived and combined with the stabilizing stage cost of the MPC controller. The resulting strategy drives the vehicle through energy efficient trajectories around the desired one. The distance between the closed-loop trajectories and the desired one provided by the user is guaranteed to be ultimately bounded. Numerical results show the effectiveness of the proposed control strategy for the case of a car driven through flat land or mountainous territory.

I. INTRODUCTION

This paper addresses the energy efficient trajectory tracking control problem for car-like vehicles, by designing a controller that considers the joint minimization of a tracking error and an index of consumption of the vehicle.

In most of the literature found in the field of energy efficient control, optimization problems are set and solved targeting an energy consumption minimization. In [1], [2], [3] over-actuated vehicles are approached with a hierarchical control structure, combining a high-level dynamic Sliding Mode Control with a low-level Energy Efficient Control Allocation (EECA) scheme which explicitly considers torque-dependent efficiency functions. In [4] these techniques are tested with the implementation of a longitudinal speed tracking controller in an electric ground vehicle, comparing adaptive, KKT-based and rule-based EECA. Another one-dimensional motion case is considered in [5], where constrained optimal control problems are first formulated to maximize the cruising range of the ground vehicle modeled in [6] and minimize its traveling time, and are then approximated and reformulated in a nonlinear parametric optimization form, which is simpler to solve. The problem of driving a wheeled robot from one point to another on a two-dimensional plane is approached in [7], by employing the A^* algorithm to find the energetically optimal path. The problem of online minimum-energy trajectory planning on a straight line path for three wheeled omni-directional mobile robots is presented in [8], with an efficient algorithm based

on Pontryagin's minimum principle, designed to minimize the energy drawn from the batteries. All these approaches deal with the consumption minimization question, using it as a unique objective function.

This paper adopts a dual target approach, with the aim to jointly minimize the vehicle consumption and the tracking error. The design is performed considering an under-actuated car-like vehicle and exploiting the result [9] to guarantee convergence of the tracking error to an ultimate bound with size proportional to the desired energy saving.

The structure of this paper is as follows. Section II reports some results from the literature, which are used in Section IV to design a trajectory tracking MPC for the dynamical model of a car-like vehicle presented in Section III. In Section V an effective algebraic approximation of the power consumption is derived and subsequently used to define the economic performance index. Numerical results show the effectiveness of the proposed strategy on an energy efficient trajectory tracking control of a vehicle navigating in flat land and mountainous territory.

II. BACKGROUND

In this section the definition of the MPC optimization problem is presented together with results from [10] for the design of an MPC with convergence guarantees to a steady-state using a given auxiliary control law. Thereafter the results from [9] are reported in order to combine the stage cost designed using [10] with an economic stage cost, whilst still guaranteeing ultimate boundedness of the closed-loop state trajectories.

A. MPC Optimization Problem

Consider a nonlinear continuous time system of the form

$$\dot{\mathbf{x}}(t) = \mathbf{f}(\mathbf{x}(t), \mathbf{u}(t)), \quad \forall t \geq 0, \quad \mathbf{x}(0) = \mathbf{x}_0 \quad (1)$$

with $\mathbf{x}(t) \in \mathbb{R}^n$ as the state vector and $\mathbf{u}(t) \in \mathbb{R}^m$ as the input vector, which is constrained for all $t \geq 0$ as $\mathbf{u}(t) \in \mathcal{U} \subseteq \mathbb{R}^m$, where \mathcal{U} denotes the input constraint set. To define the MPC optimization problem $\mathcal{P}(\mathbf{z})$, the trajectory considered on the time interval $[t_1, t_2]$ is denoted by $\mathbf{x}([t_1, t_2])$, whereas the notation $\mathbf{x}(\cdot; \mathbf{z})$ is used to show the explicit dependence of the state trajectory on the optimization parameter \mathbf{z} . For the sake of simplicity, the dependence on time is dropped whenever it is clear from the context.

Definition 1 (Open Loop MPC Problem):

Given a vector \mathbf{z} and the horizon length $T > 0$, the open-loop MPC optimization problem $\mathcal{P}(\mathbf{z})$ consists in finding

¹ Institute for Dynamic Systems and Control (IDSC), ETH Zürich, Zürich, Switzerland. maurosalar@idsc.mavt.ethz.ch

² École Polytechnique Fédérale de Lausanne (EPFL), Lausanne, Switzerland. colin.jones@epfl.ch

³ Institute for Systems and Robotics (ISR), Instituto Superior Tecnico (IST), Lisbon, Portugal.

⁴ Faculty of Engineering, University of Porto (FEUP), Porto, Portugal. pedro.aguiar@fe.up.pt

the optimal control trajectory $\bar{\mathbf{u}}^*([0, T])$ that solves

$$\begin{aligned} J_T^* &= \min_{\bar{\mathbf{u}}([0, T])} J_T(\mathbf{z}, \bar{\mathbf{u}}([0, T])) \\ \text{s.t. } \dot{\bar{\mathbf{x}}}(\tau) &= \mathbf{f}(\bar{\mathbf{x}}(\tau), \bar{\mathbf{u}}(\tau)), \quad \forall \tau \in [0, T] \\ \bar{\mathbf{x}}(0) &= \mathbf{z}, \quad \bar{\mathbf{x}}(T) \in \mathcal{X}_a \\ \bar{\mathbf{u}}(\tau) &\in \mathcal{U}, \quad \forall \tau \in [0, T], \end{aligned}$$

where

$$J_T(\mathbf{z}, \bar{\mathbf{u}}([0, T])) = \underbrace{\int_0^T l(\bar{\mathbf{x}}(\tau), \bar{\mathbf{u}}(\tau)) d\tau}_{\text{Finite horizon cost}} + \underbrace{m(\bar{\mathbf{x}}(T))}_{\text{Terminal cost}}.$$

The *finite horizon cost* $J_T(\cdot)$ is composed by the *stage cost* $l : \mathbb{R}^n \times \mathbb{R}^m \rightarrow \mathbb{R}_+$, and the *terminal cost* $m : \mathbb{R}^n \rightarrow \mathbb{R}_+$, defined over the *auxiliary terminal set* $\mathcal{X}_a \subseteq \mathbb{R}^n$. The stage cost is decomposed as

$$l(\mathbf{x}, \mathbf{u}) = \underbrace{l_s(\mathbf{x}, \mathbf{u})}_{\text{stabilizing stage cost}} + \underbrace{l_e(\mathbf{x}, \mathbf{u})}_{\text{economic stage cost}}, \quad (2)$$

where the *stabilizing stage cost* $l_s : \mathbb{R}^n \times \mathbb{R}^m \rightarrow \mathbb{R}_+$ is the one used in Tracking MPC to enforce convergence to the chosen equilibrium point, and the *economic stage cost* $l_e : \mathbb{R}^n \times \mathbb{R}^m \rightarrow \mathbb{R}$ is an arbitrary function that we would also like to minimize. Given that the system is time invariant, the open-loop state and input trajectories are considered, without loss of generality, over the interval $[0, T]$. We denote by $\mathbf{k}_a : \mathcal{X}_a \rightarrow \mathcal{U}$ a feasible *auxiliary control law* defined over the terminal set. In a sampled-data approach the *MPC control law* is defined as

$$\mathbf{u}(t) = \mathbf{k}_{\text{MPC}}(\mathbf{x}(t)) := \bar{\mathbf{u}}^*(t - [t]; \mathbf{x}([t])), \quad (3)$$

where $[t] := \max\{t_i \in \mathcal{T} : t_i \leq t\}$.

B. Stable MPC with an Auxiliary Control Law

Consider the following results from [10], where the assumptions for convergence to a steady-state of the Tracking MPC are recovered using $l_e(\cdot) = 0$, $\lambda(\cdot) = 0$, and $l_s(\mathbf{0}, \mathbf{0}) = 0$. Moreover, we consider $\mathcal{X} = \mathbb{R}^n$.

Assumption 1: $\mathbf{f}(\cdot)$ is locally Lipschitz continuous in the region of interest and $\mathbf{f}(\mathbf{0}, \mathbf{0}) = \mathbf{0}$. \square

Assumption 2: The optimization problem $\mathcal{P}(\mathbf{x}_0)$ admits a feasible solution. \square

Assumption 3 (Sufficient Conditions for Convergence):

- (i) The sets $\mathcal{X}_a \subseteq \mathbb{R}^n$ and $\mathcal{U} \subseteq \mathbb{R}^m$ are compact and $(\mathbf{0}, \mathbf{0}) \in \text{int}(\mathcal{X}_a) \times \text{int}(\mathcal{U})$.
- (ii) The stage cost is lower bounded by a class \mathcal{K}_∞ function $\alpha(\cdot)$, i.e. $\alpha(\|\mathbf{x}\|) \leq l_s(\mathbf{x}, \mathbf{u}), \forall (\mathbf{x}, \mathbf{u}) \in \mathbb{R}^n \times \mathcal{U}$.
- (iii) The function $m(\cdot)$ is positive semi-definite and continuously differentiable away from the origin.
- (iv) There exists a feasible control law $\mathbf{k}_a : \mathbb{R}^n \rightarrow \mathbb{R}^m$, defined over the terminal set \mathcal{X}_a , such that, for the closed-loop system (1) with $\mathbf{u}(t) = \mathbf{k}_a(\mathbf{x})$, the state and input vectors are such that $\mathbf{x}(t) \in \mathcal{X}_a$ and $\mathbf{u}(t) \in \mathcal{U}$, respectively, and the cost decrease condition $\dot{m}(\mathbf{x}) = \frac{\partial}{\partial \mathbf{x}} \mathbf{f}(\mathbf{x}, \mathbf{u}) \leq -l_s(\mathbf{x}, \mathbf{k}_a(\mathbf{x}))$ holds for all the $\mathbf{x} \neq \mathbf{0}$ and $\mathbf{x}_0 \in \mathcal{X}_a$. \square

Assumption 4 (Known auxiliary law): Suppose that a feasible control law $\mathbf{k}_a : \mathcal{X}_a \rightarrow \mathcal{U}$ together with a certificate

of exponential stability of the origin of the closed-loop system with $\mathbf{u}(t) = \mathbf{k}_a(t, \mathbf{x}) \in \mathcal{U}$ are given. Let the certificate be a continuously differentiable Lyapunov function $V_a : \mathbb{R}^n \rightarrow \mathbb{R}_+$, with the positive constants k_1, k_2, k_3 and a such that $k_1 \|\mathbf{x}\|^a \leq V_a(\mathbf{x}) \leq k_2 \|\mathbf{x}\|^a$, $\frac{d}{dt} V_a(\mathbf{x}) \leq -k_3 \|\mathbf{x}\|^a$ hold for all $\mathbf{x} \in \mathcal{X}_a := \mathcal{L}(V_a, r) = \{\mathbf{x} : V_a(\mathbf{x}) \leq r\}$ with $r \geq 0$. \square

Assumption 5 (Bound on stage cost): The control law from Assumption 4 and the stage cost $l_s(\cdot)$ are such that $l_s(\mathbf{x}, \mathbf{k}_a(\mathbf{x})) \leq \sum_{i=1}^v a_i \|\mathbf{x}\|^i$, $\forall \mathbf{x} \in \mathcal{X}_a$, where $v \in \mathbb{N}^*$ and $a_i \in \mathbb{R}$.

Proposition 1: Consider system (1) in closed-loop with the auxiliary control law from Assumption 4 and let Assumption 5 hold. Then, the terminal cost function

$$m(\mathbf{x}) = \sum_{i=1}^v a_i \left(\frac{k_2}{k_1} \right)^{i/a} \frac{ak_2}{ik_3} \|\mathbf{x}\|^i$$

and the terminal state \mathcal{X}_a satisfy Assumption 3 (iii)-(iv). \square The Assumptions 1-3 are the ones used in Tracking MPC ($l_e(\cdot) = 0$), to show convergence to the origin.

Theorem 1 (Convergence of Tracking MPC, e.g., [10]): Consider the constrained system (1) in closed-loop with (3) and suppose that Assumptions 1-3 hold. Then, the state vector $\mathbf{x}(t)$ converges to $\mathbf{0}$ as $t \rightarrow \infty$ with region of attraction consisting of the set of states \mathbf{x} for which $\mathcal{P}(\mathbf{x})$, introduced in Definition 1, admits a feasible solution. \square

C. Ultimately Bounded MPC with Economic Stage Cost

The following assumption and theorem are taken from [9].

Assumption 6 (Bound on the Economic Stage Cost):

The norm of the economic stage cost $l_e(\cdot)$, evaluated along the closed-loop state and input trajectories, is uniformly bounded by a strictly positive constant value, i.e. $\|l_e(\mathbf{x}(t), \mathbf{u}(t))\| \leq B, \forall t \geq 0$ with $B > 0$. \square

Theorem 2 (Ultimate Boundedness): Consider system (1) in closed-loop with (3), where $l(\cdot)$ is decomposed as in (2), and suppose Assumptions 1-3 and 6 hold. Then, for every \mathbf{x}_0 that satisfies Assumption 2 the closed-loop state trajectory is uniformly bounded over time, i.e. $\|\mathbf{x}(t)\| \leq c \in \mathbb{R}_+, \forall t \geq 0$, and converges to an ultimate bound with size proportional to the value of B from Assumption 6, i.e. there exists a finite time $\bar{T} \geq 0$ and a constant $U > 0$ such that

$$\|\mathbf{x}(t)\| \leq U, \forall t \geq \bar{T}, \quad (4)$$

where for every desired value of $U > 0$ there exists a bound $B > 0$ so that (4) holds. \square

III. VEHICLE MODEL

In this section, a dynamical model of a car-like vehicle is presented.

A. Equation of Motion

A common model used to describe car-like vehicles, which shares the same kinematic properties, is the bicycle model shown in Fig. 1 (e.g. [11], page 26, Table 2.1). The kinematic model has as state variables the position of the center of mass in the inertial reference frame $\mathbf{p} = (x, y)^T$, the orientation

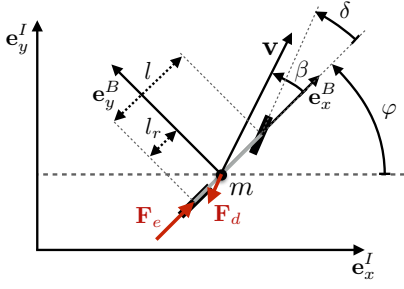


Fig. 1. Graphic representation of the bicycle model.

of the vehicle φ and the steering angle δ , which can be replaced by the slip-angle $\beta = \tan^{-1}\left(\frac{l_r}{l} \tan(\delta)\right)$, where the distances l_r and l are defined in Fig. 1. The dynamical model is derived neglecting the inertia of the system, considering the non-holonomic constraints between wheels and ground, and including the velocity of the center of mass v as an additional variable and its acceleration a as input. The state equations of the system can be described by

$$\begin{aligned} \dot{\mathbf{p}} &= \mathbf{R}(\mathbf{x}) \begin{pmatrix} v \\ 0 \end{pmatrix}, & \dot{\varphi} &= \frac{v}{l_r} \sin \beta, \\ \dot{v} &= u_1, & \dot{\beta} &= u_2, \end{aligned} \quad (5)$$

with state vector $\mathbf{x} = (x, y, \varphi, v, \beta)^T$, control input $\mathbf{u} = (a, \dot{\beta})^T$ and rotation matrix defined as

$$\mathbf{R}(\mathbf{x}) = \begin{pmatrix} \cos(\varphi + \beta) & -\sin(\varphi + \beta) \\ \sin(\varphi + \beta) & \cos(\varphi + \beta) \end{pmatrix}.$$

Note that the model (5) does not explicitly consider the forces acting on the vehicle. However, they can be obtained from the state and input vector, as shown in the subsequent section.

B. Drag Forces and Electric Propulsion

Consider the case where the vehicle is powered by a DC electric motor. From [12], the motor current I is governed by the following dynamical equation

$$\dot{I} = -\frac{R}{L}I - \frac{\kappa\lambda}{Lr_w}v \cos(\beta) + \frac{1}{L}U_m,$$

where $L > 0$ denotes the internal inductance, $R_c > 0$ the internal resistance, $\kappa > 0$ the current-to-torque constant, $U_m \in \mathbb{R}$ the applied voltage, $\lambda \geq 1$ the gear ratio, and $r_w > 0$ the wheel radius. Then, the driving force on the rear wheels can be described by $F_e = \frac{\kappa\lambda}{r_w}I$. The acceleration of the vehicle is $a = \frac{1}{m}(F_e \cos(\beta) - F_d)$, where the drag force F_d consists of rolling friction F_r , gravitational force F_g and aerodynamic drag F_a , [12]. The rolling friction is modeled as $F_r = k_0 \frac{2}{\pi} \arctan\left(\frac{v}{k_R}\right)$. Considering a vehicle moving on a plane parametrized by $(x, y, h(x, y))$, the gravitational force can be obtained as $F_g = mg \sin(\alpha)$, where

$$\alpha(x, y, \varphi, \beta) = \arctan\left(\left(\begin{pmatrix} \cos(\varphi + \beta) \\ \sin(\varphi + \beta) \end{pmatrix}\right)^T \nabla h(x, y)\right).$$

The aerodynamic drag is neglected. Hence the total drag force is $F_d(x, y, \varphi, v, \beta) = F_r(v) + F_g(x, y, \varphi, \beta)$.

IV. MPC FOR TRAJECTORY TRACKING

In this section a trajectory tracking MPC is derived for the car-like vehicle model (5) presented in Section III-A. More precisely, first by using backstepping we compute a nonlinear auxiliary control law that stabilizes exponentially fast to the origin of an error space. Then the exponential stability properties of the auxiliary control law are exploited, as illustrated in Section II-B, to design a trajectory tracking MPC with convergence guarantees of the error vector to zero.

A. Auxiliary Law

Assuming a twice differentiable desired trajectory $\mathbf{p}_d: \mathbb{R}_+ \rightarrow \mathbb{R}^2$, we define the following rotated tracking error

$$\mathbf{e} := \mathbf{R}(\mathbf{x})^T(\mathbf{p}(\mathbf{x}) - \mathbf{p}_d(t)) + \boldsymbol{\varepsilon},$$

where $\boldsymbol{\varepsilon} := (\varepsilon_1, \varepsilon_2)^T$.

Lemma 1: Consider the system (5) in closed-loop with the auxiliary control law

$$\begin{aligned} \mathbf{k}_a(t, \mathbf{e}(t, \mathbf{x}), \zeta(t, \mathbf{x})) &= \\ &= \begin{pmatrix} \left((-1, 0) + \begin{pmatrix} 1, \frac{\varepsilon_2}{\varepsilon_1} \end{pmatrix} \mathbf{K} \mathbf{S}(\omega) \right) \mathbf{e} - k_\zeta \zeta + q_2 \\ -\frac{v}{l_r} \sin(\beta) + \begin{pmatrix} 0, \frac{1}{\varepsilon_1} \end{pmatrix} (-\mathbf{K} \mathbf{e} + \mathbf{R}^T \dot{\mathbf{p}}_d) \end{pmatrix}, \end{aligned} \quad (6)$$

where

$$\begin{aligned} \zeta &:= v - [\Delta^{-1}]_1 (-\mathbf{K} \mathbf{e} + \mathbf{R}^T \dot{\mathbf{p}}_d) \\ q_2 &:= [\Delta^{-1}]_1 (-\mathbf{K}(\mathbf{S}(\omega) \boldsymbol{\varepsilon} + (v, 0)^T - \mathbf{R}^T \dot{\mathbf{p}}_d) \\ &\quad - \mathbf{S}(\omega) \mathbf{R}^T \dot{\mathbf{p}}_d + \mathbf{R}^T \dot{\mathbf{p}}_d) \\ \Delta &:= \begin{pmatrix} 1 & -\varepsilon_2 \\ 0 & \varepsilon_1 \end{pmatrix}, \quad \mathbf{S}(\omega) := \begin{pmatrix} 0 & -\omega \\ \omega & 0 \end{pmatrix} \\ \omega &:= \frac{v}{l_r} \sin(\beta) + u_2, \quad \hat{\mathbf{e}} := (\mathbf{e}^T, \zeta)^T \\ \mathbf{K} &= \mathbf{K}^T \text{ positive definite, } \boldsymbol{\varepsilon} \in \mathbb{R}_+^* \times \mathbb{R}_+. \end{aligned}$$

Then, the origin of the augmented error space $\hat{\mathbf{e}}^* = \mathbf{0}$ is globally exponentially stable. \square

Proof: It can be shown that $\dot{\mathbf{R}}^T = -\mathbf{S}(\omega) \mathbf{R}^T$, where $\mathbf{S}(\cdot)$ is the skew-symmetric matrix operator defined as

$$\mathbf{S}(\omega) = \begin{pmatrix} 0 & -\omega \\ \omega & 0 \end{pmatrix}$$

and $\omega := \dot{\varphi} + \dot{\beta} = \frac{v}{l_r} \sin(\beta) + u_2$. Thus the error dynamics

$$\begin{aligned} \dot{\mathbf{e}} &= -\mathbf{S}(\omega) \mathbf{R}^T(\mathbf{p} - \mathbf{p}_d) + \mathbf{R}^T(\dot{\mathbf{p}} - \dot{\mathbf{p}}_d) = \\ &= -\mathbf{S}(\omega) \underbrace{(\mathbf{R}^T(\mathbf{p} - \mathbf{p}_d) + \boldsymbol{\varepsilon})}_{\mathbf{e}} + \underbrace{\mathbf{R}^T \dot{\mathbf{p}}}_{(v, 0)^T} - \mathbf{R}^T \dot{\mathbf{p}}_d + \underbrace{\mathbf{S}(\omega) \boldsymbol{\varepsilon}}_{(-\varepsilon_2, \varepsilon_1)^T \omega} = \\ &= -\mathbf{S}(\omega) \mathbf{e} + \underbrace{\begin{pmatrix} 1 & -\varepsilon_2 \\ 0 & \varepsilon_1 \end{pmatrix}}_{=\Delta} \begin{pmatrix} v \\ \omega \end{pmatrix} - \mathbf{R}^T \dot{\mathbf{p}}_d. \end{aligned}$$

Consider the candidate Lyapunov function of the form $V(\mathbf{e}) = \frac{1}{2} \mathbf{e}^T \mathbf{e}$. In order to have a total time derivative of the form $\dot{V}(\mathbf{e}) = \mathbf{e}^T \dot{\mathbf{e}} = -\mathbf{e}^T \mathbf{K} \mathbf{e}$, with $\mathbf{K} = \mathbf{K}^T$ positive definite, one would like to choose

$$\begin{pmatrix} v \\ \omega \end{pmatrix} = \Delta^{-1} (-\mathbf{K} \mathbf{e} + \mathbf{R}^T \dot{\mathbf{p}}_d) = \begin{pmatrix} [\Delta^{-1}]_1 \\ [\Delta^{-1}]_2 \end{pmatrix} (-\mathbf{K} \mathbf{e} + \mathbf{R}^T \dot{\mathbf{p}}_d),$$

where $[\mathbf{M}]_i$ denotes the i -th row of the matrix \mathbf{M} . Notice that $\omega = \frac{v}{l_r} \sin(\beta) + u_2$ and therefore the second input can be chosen as

$$u_2 = -\frac{v}{l_r} \sin(\beta) + [\Delta^{-1}]_2 (-\mathbf{K}\mathbf{e} + \mathbf{R}^T \dot{\mathbf{p}}_d) .$$

Since the term v has its own dynamics and cannot be directly determined by the input, we proceed in a backstepping fashion by defining the backstepping variable

$$\zeta := v - [\Delta^{-1}]_1 (-\mathbf{K}\mathbf{e} + \mathbf{R}^T \dot{\mathbf{p}}_d)$$

with total time derivative

$$\dot{\zeta} := u_1 - \underbrace{[\Delta^{-1}]_1 (-\mathbf{K}\dot{\mathbf{e}} - \mathbf{S}(\omega)\mathbf{R}^T \dot{\mathbf{p}}_d + \mathbf{R}^T \ddot{\mathbf{p}}_d)}_{=:q_1} .$$

Considering the new Lyapunov function candidate

$$V_a(\mathbf{e}, \zeta) = \frac{1}{2} (\mathbf{e}^T \mathbf{e} + \zeta^2) ,$$

with first derivative

$$\begin{aligned} \dot{V}_a(\mathbf{e}, \zeta) &= \mathbf{e}^T \dot{\mathbf{e}} + \zeta \dot{\zeta} \\ &= \mathbf{e}^T \left(-\mathbf{S}(\omega)\mathbf{e} - \mathbf{R}^T \dot{\mathbf{p}}_d + \underbrace{\Delta \begin{pmatrix} v \\ \omega \end{pmatrix}}_{-\mathbf{K}\mathbf{e} + \mathbf{R}^T \dot{\mathbf{p}}_d + (\zeta, 0)^T} \right) \\ &\quad + \zeta (u_1 - q_1) = -\mathbf{e}^T \mathbf{K}\mathbf{e} + \zeta (u_1 - q_1 + [\mathbf{e}]_1) \end{aligned}$$

combined with $u_1 - q_1 + [\mathbf{e}]_1 = -k_\zeta \zeta$, where $q_1 = [\Delta^{-1}]_1 (-\mathbf{K}\dot{\mathbf{e}} - \mathbf{S}(\omega)\mathbf{R}^T \dot{\mathbf{p}}_d + \mathbf{R}^T \ddot{\mathbf{p}}_d)$, results in

$$\dot{V}_a(\mathbf{e}, \zeta) = -\mathbf{e}^T \mathbf{K}\mathbf{e} - k_\zeta \zeta^2 ,$$

which is negative definite and ensures global exponential stability of $\hat{\mathbf{e}}^* = ((\mathbf{e}^*)^T, \zeta^*)^T = \mathbf{0}$, thus concluding the proof. ■

B. MPC Control Law

Building on the auxiliary control law derived in the previous section and using the results from Section II-B, here we proceed to design an MPC control law that drives the vector $\hat{\mathbf{e}}$ to the origin. Thus, the results from the background section are considered on the augmented error vector $\hat{\mathbf{e}}$, as it is done in [13] for the unicycle.

C. Stabilizing Stage Cost

The stabilizing stage cost is chosen as

$$l_s(\hat{\mathbf{e}}, \mathbf{u}) = \|\hat{\mathbf{e}}(t, \mathbf{x})\|_{\mathbf{Q}}^2 + \|\mathbf{u}(t) - \mathbf{k}_a(t, \hat{\mathbf{e}}(t, \mathbf{x}))\|_{\mathbf{T}}^2 , \quad (7)$$

where $\mathbf{k}_a(t, \hat{\mathbf{e}})$ is defined in equation (6), and $\|\hat{\mathbf{e}}\|_{\mathbf{Q}}^2 := \hat{\mathbf{e}}^T \mathbf{Q} \hat{\mathbf{e}}$ with $\mathbf{Q} = \mathbf{Q}^T$ positive definite and $\mathbf{T} = \mathbf{T}^T$ positive semidefinite.

D. Terminal Cost

The Lyapunov function $V_a(\cdot)$ satisfies Assumption 4 with $k_1 = k_2 = 1/2$, $a = 2$ and $k_3 = \max\{\lambda_{\max}(\mathbf{K}), k_\zeta\}$ and the stabilizing stage cost satisfies Assumption 5 with $v = 2$, $a_1 = 0$ and $a_2 = \lambda_{\max}(\mathbf{Q})$, therefore, applying Proposition 1 results in the terminal cost as

$$m(\hat{\mathbf{e}}) = \frac{\lambda_{\max}(\mathbf{Q})}{2 \max\{\lambda_{\max}(\mathbf{K}), k_\zeta\}} \|\hat{\mathbf{e}}\|^2 . \quad (8)$$

E. Input Constraint Sets

The input constraint set is chosen to be

$$\mathcal{U} = \left[-a_0 \left(1 + \frac{v}{v_{\max}} \right), a_0 \left(1 - \frac{v}{v_{\max}} \right) \right] \times \left[-\dot{\beta}_{\max}, \dot{\beta}_{\max} \right] , \quad (9)$$

whose first component has the form of the speed-to-torque lines of a DC motor and guarantees $v(t) \in [-v_{\max}, v_{\max}] \forall v_0 \in [-v_{\max}, v_{\max}]$.

F. Terminal State Constraint Set

In order to satisfy Assumption 4 and exploit the convergence guarantees of Theorem 1 from [10], the terminal set is chosen to be a sublevel set of the Lyapunov function with feasible associated state and input closed-loop trajectories. $\mathcal{X}_a(t)$ is built implicitly, by constructing a terminal set for $\hat{\mathbf{e}}(t, \mathbf{x})$ as $\mathcal{E}_a := \{\hat{\mathbf{e}}(t, \mathbf{x}) : V_a(\hat{\mathbf{e}}) \leq r, \mathbf{k}_a(t, \hat{\mathbf{e}}) \in \mathcal{U}\}$ for some $r \in \mathbb{R}_+$. Consider the system in closed-loop with the auxiliary control law. Ideally, we would like to compute the largest level set $\mathcal{L}(V_a, r)$ with feasible associated state and input closed-loop trajectory, i.e. with

$$r = \max\{\bar{r} \geq 0 : \mathbf{k}_a(t, \hat{\mathbf{e}}) \in \mathcal{U}, \forall \hat{\mathbf{e}} \in \mathcal{L}(V_a, \bar{r}), t \geq 0\} .$$

Note that the condition $\mathbf{k}_a(\hat{\mathbf{e}}) \in \mathcal{U}$ can be rewritten by combining (9) with (6), as

$$\begin{aligned} &((-1, 0) + [\Delta^{-1}]_1 \mathbf{K}\mathbf{S}(\omega)) \mathbf{e} - k_\zeta \zeta + q_2 + \\ &\quad + a_0 \frac{v}{v_{\max}} \in [-a_0, a_0] \\ &\quad - \frac{v}{l_r} \sin(\beta) + [\Delta^{-1}]_2 (-\mathbf{K}\mathbf{e} + \mathbf{R}^T \dot{\mathbf{p}}_d) \in \left[-\dot{\beta}_{\max}, \dot{\beta}_{\max} \right] . \end{aligned} \quad (10)$$

In order to make the inequalities (10) only dependent on the vector $\hat{\mathbf{e}}$, we proceed by bounding the components that are function of time and state. Consider the maximal velocity v_{\max} , the maximal desired velocity $v_{d, \max} = \max_t \{\|\dot{\mathbf{p}}_d(t)\|\}$ and the maximal desired acceleration $a_{d, \max} := \max_t \{\|\ddot{\mathbf{p}}_d(t)\|\}$. Then, the first input constraint of (10) can be upper-bounded as

$$\begin{aligned} &((-1, 0) + [\Delta^{-1}]_1 \mathbf{K}\mathbf{S}(\omega)) \mathbf{e} - k_\zeta \zeta + \\ &\quad + [\Delta^{-1}]_1 \left(-\mathbf{K}\mathbf{S}(\omega)\mathbf{e} + \mathbf{K}\mathbf{R}^T \dot{\mathbf{p}}_d + \mathbf{R}^T \ddot{\mathbf{p}}_d - \mathbf{S}(\dot{\beta})\mathbf{R}^T \dot{\mathbf{p}}_d \right) + \\ &\quad + \left([\Delta^{-1}]_1 \left(-\mathbf{K}(1, 0)^T - \mathbf{S}(1)\mathbf{R}^T \dot{\mathbf{p}}_d \frac{1}{l_r} \right) + \frac{a_0}{v_{\max}} \right) v \\ &\quad \leq k_v := |[\Delta^{-1}]_1 \mathbf{K}(1, 0)^T| + \|[\Delta^{-1}]_1\| \frac{v_{d, \max}}{l_r} + \frac{a_0}{v_{\max}} \\ &\in [-a_0, a_0] , \end{aligned} \quad (11)$$

Combining (11) with $v = \zeta + [\Delta^{-1}]_1 (-\mathbf{K}\mathbf{e} + \mathbf{R}^T \dot{\mathbf{p}}_d)$, $\omega_{\max} = v_{\max}/l_r + \dot{\beta}_{\max}$, $\|\mathbf{R}^T \dot{\mathbf{p}}_d\| \leq v_{d, \max}$ and $\|\mathbf{R}^T \ddot{\mathbf{p}}_d\| \leq a_{d, \max}$ leads to

$$\begin{aligned} &\underbrace{\left(\|[\Delta^{-1}]_1 \mathbf{K}\mathbf{S}(\omega_{\max})\| + \|[\Delta^{-1}]_1 \mathbf{K}\mathbf{k}_v\| + 1 \right)}_{=: \gamma} \|\mathbf{e}\| + \\ &\quad + (k_v + k_\zeta) |\zeta| \leq a_0 - \|[\Delta^{-1}]_1 \mathbf{K}\mathbf{S}(\omega_{\max})\mathbf{e}\| \\ &\quad - \left(\|[\Delta^{-1}]_1\| k_v + \|[\Delta^{-1}]_1 \mathbf{K}\| + \|[\Delta^{-1}]_1 \mathbf{S}(\dot{\beta}_{\max})\| \right) v_{d, \max} \\ &\quad - \|[\Delta^{-1}]_1\| a_{d, \max} =: b_1 . \end{aligned} \quad (12)$$

Note that the set induced by (12), i.e. $\{\hat{\mathbf{e}} : (12)\}$, contains the ellipsoid $\mathcal{S}_1 := \{\hat{\mathbf{e}} : \hat{\mathbf{e}}^T \mathbf{P}_1 \hat{\mathbf{e}} \leq b_1^2\}$, where $\mathbf{P}_1 := \text{diag}\{\gamma^2, \gamma^2, (k_v + k_\zeta)^2\}$. We perform this approximation, because it is easier to look for the largest r , such that $\mathcal{L}(V_a, r) \subseteq \mathcal{S}_1$, i.e.

$$r_1 = \max_r \{r \geq 0 : \mathcal{L}(V_a, r) \subseteq \mathcal{S}_1\} = \frac{1}{2} \left(\frac{b_1}{\max\{\gamma, k_v + k_\zeta\}} \right)^2.$$

The same approach is used for the second input constraint. Inserting $v = \zeta + [\Delta^{-1}]_1(-\mathbf{K}\mathbf{e} + \mathbf{R}^T \dot{\mathbf{p}}_d)$ in the second inclusion of (10), we obtain

$$\begin{aligned} & \left(\frac{\sin(\beta)}{l_r}, -1 \right) \Delta^{-1} \mathbf{K}\mathbf{e} - \frac{\sin(\beta)}{l_r} \zeta \\ & - \left(\frac{\sin(\beta)}{l_r}, -1 \right) \Delta^{-1} \mathbf{R}^T \dot{\mathbf{p}}_d \in [-\dot{\beta}_{\max}, \dot{\beta}_{\max}]. \end{aligned}$$

In order to have a simpler form, where β is not present, we use the fact that

$$\left\| \left(\frac{\sin(\beta)}{l_r}, -1 \right) \Delta^{-1} \right\| \leq \left\| \left(\frac{-1}{l_r}, -1 \right) \Delta^{-1} \right\|,$$

for $\varepsilon_1 > 0$ and $\varepsilon_2 \geq 0$, and $\|\mathbf{R}^T \dot{\mathbf{p}}_d\| \leq v_{d,\max}$, leading to the search of the largest $\mathcal{L}(V_a, r)$ contained in the polytope

$$\mathcal{P}_2 := \left\{ \hat{\mathbf{e}} : \left(-\left(\frac{c_1}{l_r}, 1 \right) \Delta^{-1} \mathbf{K}, \frac{c_2}{l_r} \right) \hat{\mathbf{e}} \in [-b_2, b_2], \right. \\ \left. c_1, c_2 \in \{-1, 1\} \right\},$$

where $b_2 := \dot{\beta}_{\max} - \left\| \left(\frac{-1}{l_r}, -1 \right) \Delta^{-1} \right\| v_{d,\max}$ and we use the fact that $[-b_2, b_2]$ is convex and $\sin(\beta) \in [-1, 1]$. The optimization problem

$$r_2 = \max_r \{r \geq 0 : \mathcal{L}(V_a, r) \subseteq \mathcal{P}_2\},$$

is equivalent to the geometric problem of finding the largest ellipsoid $1/2\hat{\mathbf{e}}^T \hat{\mathbf{e}} \leq r_2$ inscribed in the polytope \mathcal{P}_2 , which has a closed form solution (see e.g. [14]). The feasibility of the auxiliary control law is ensured by choosing $r := \min\{r_1, r_2\}$, which results in the terminal set

$$\mathcal{X}_a(t) = \{\mathbf{x} \in \mathbb{R}^n : V_a(\hat{\mathbf{e}}(t, \mathbf{x})) \leq r\}. \quad (13)$$

V. ECONOMIC MPC

The EMPC is designed by augmenting the stabilizing stage cost $l_s(\cdot)$ of the stable MPC obtained in Section IV with an economic stage cost $l_e(\cdot)$. In order to use the results of [9], reported in Section II-C, and thus guarantee ultimate boundedness of the error trajectories, we need to fulfill Assumption 6. Observe that Assumptions 1-3 are satisfied with the designed stabilizing stage cost (7), terminal cost (8) and terminal set (13). The economic stage cost is chosen to be the power extracted from the battery $P_b = \eta_b P_{DC}$, where the motor power is $P_{DC} = U_m I$ and the battery efficiency is $\eta_b = \frac{1}{\eta_d}$ if $P_{DC} \geq 0$ (discharge), η_c if $P_{DC} < 0$ (charge). Assuming fast motor dynamics, i.e. $L \approx 0$, the current and the voltage can be described by the algebraic functions $I = \frac{r_w}{\kappa \lambda} F_e$

and $U_m = \frac{R_c r_w}{\kappa \lambda} F_e + \frac{\kappa \lambda}{r_w} v \cos(\beta)$, where $F_e = \frac{ma + F_d(\mathbf{x})}{\cos(\beta)}$. From this,

$$P_{DC}(\mathbf{x}, \mathbf{u}) = \underbrace{R_c \left(\frac{r_w(ma + F_d(\mathbf{x}))}{\kappa \lambda \cos(\beta)} \right)^2}_{\text{Resistance Power}} + \underbrace{(ma + F_d(\mathbf{x}))v}_{\text{Mechanical Power}}. \quad (14)$$

It can be shown that the chosen approximation well describes the real behavior of the motor. Finally, the motor power can be combined with the battery efficiency to get the power extracted from the battery, which is used to design the economic stage cost as

$$l_e(\mathbf{x}, \mathbf{u}) = \alpha_e P_b(\mathbf{x}, \mathbf{u}) = \alpha_e P_{DC}(\mathbf{x}, \mathbf{u}) \eta_b, \quad (15)$$

with α_e as the weighting factor used to tune the importance of the power consumption in the MPC optimization algorithm. Recall that (15) satisfies Assumption 6, as P_{DC} is bounded along the closed-loop state and input trajectories.

VI. SIMULATIONS

Simulations are made considering a radio controlled electric car without kinetic energy recovery system (i.e. $\eta_c = 0$ and $\eta_d = 1$). The nonlinear solver ACADO [15] is employed, and the simulator is implemented in MATLAB. Two scenarios are chosen: a flat surface and a smooth surface with a hill. In both cases the desired trajectory has the sinusoidal form $\mathbf{p}_d(t) = (v_{d,x} t, A \sin(vt))^T$. First, the stable MPC is implemented, setting $\alpha_e = 0$. Subsequently this weight is stepwise increased and at each step the simulation is repeated.

A. Slalom on a Flat Surface

The results of the trajectory tracking simulation on the flat surface are shown below. In Fig. 2, the desired and real trajectories are shown for different values of α_e , whereas in Fig. 3 the mean error and the mean power consumption are plotted as a function of the weight α_e of the economic stage cost.

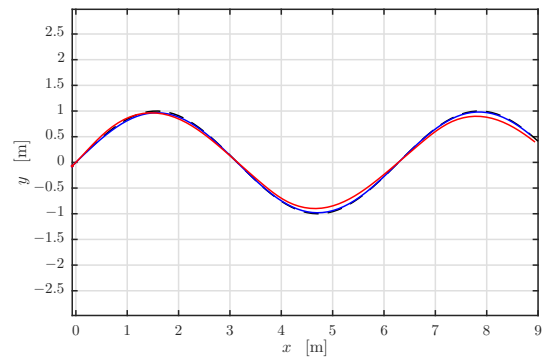


Fig. 2. Desired trajectory (black dashed) and vehicle trajectories with $\alpha_e = 0$ (blue solid) and $\alpha_e = 0.7$ (red solid).

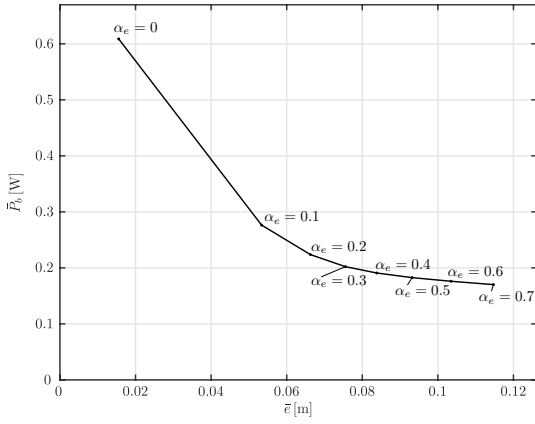


Fig. 3. Mean tracking error and battery power.

B. Slalom on a Mountainous Surface

For this set of simulations a mound is placed on the desired trajectory and therefore the gravity force plays an important role in the energy consumption of the vehicle. As Fig. 4 reveals, the stable MPC is not affected by this new scenario. On the other hand, the ultimately bounded EMPC chooses a trajectory along an isoline of the mound, when the gradient becomes too steep.

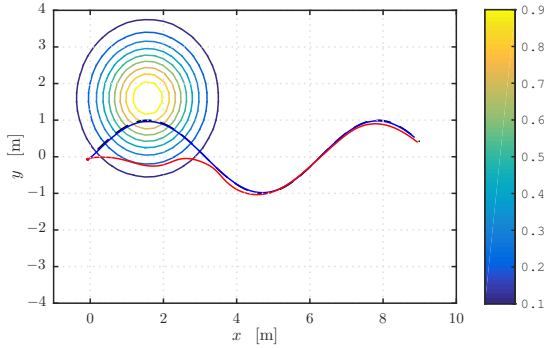


Fig. 4. Desired trajectory (black dashed) and vehicle trajectories with $\alpha_e = 0$ (blue solid) and $\alpha_e = 0.7$ (red solid) with isolines.

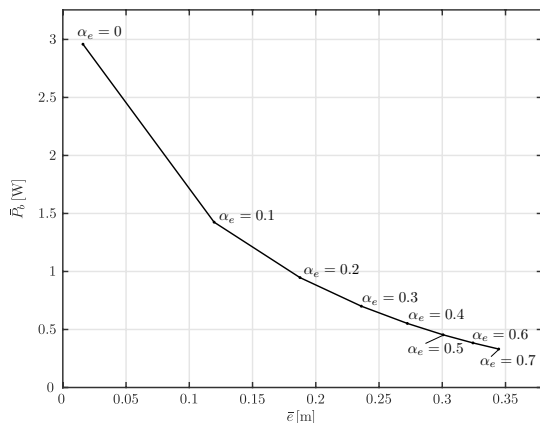


Fig. 5. Mean tracking error and battery power.

C. Discussion

In both scenarios, the use of the proposed strategy allowed to save energy while still guaranteeing closed-loop boundedness around the desired trajectory. The expected relation between energy saving and tracking error is shown in Fig. 3 and 5 for flat and mountainous territory, respectively.

VII. CONCLUSIONS

A nonlinear trajectory tracking control law for car-like vehicles was derived and used to design a stable MPC. This was then combined with an economic stage cost representing the energy consumption of a vehicle driven by electric propulsion. As expected, a higher bound on the economic stage cost, resulting from a larger weighting factor, enlarged the convergence region of the trajectory around the desired one. The resulting strategy was proved to be an effective energy efficient control algorithm with a tunable power consumption weight, which allows to get the most satisfying trade-off between tracking performance and energy saving.

REFERENCES

- [1] Y. Chen and J. Wang, "Energy-efficient control allocation with applications on planar motion control of electric ground vehicles," in *American Control Conference (ACC)*, 2011, pp. 2719–2724, IEEE, 2011.
- [2] Y. Chen and J. Wang, "Fast and global optimal energy-efficient control allocation with applications to over-actuated electric ground vehicles," *Control Systems Technology, IEEE Transactions on*, vol. 20, no. 5, pp. 1202–1211, 2012.
- [3] Y. Chen and J. Wang, "Adaptive energy-efficient control allocation for planar motion control of over-actuated electric ground vehicles," 2014.
- [4] Y. Chen and J. Wang, "Design and experimental evaluations on energy efficient control allocation methods for overactuated electric vehicles: Longitudinal motion case," *Mechatronics, IEEE/ASME Transactions on*, vol. 19, no. 2, pp. 538–548, 2014.
- [5] T. Wang and C. G. Cassandras, "Optimal motion control for energy-aware electric vehicles," in *Control Applications (CCA), 2013 IEEE International Conference on*, pp. 388–393, IEEE, 2013.
- [6] D. Tanaka, T. Ashida, and S. Minami, "An analytical method of ev velocity profile determination from the power consumption of electric vehicles," in *IEEE Vehicle Power and Propulsion Conference (VPPC)*, Harbin, China, 2008.
- [7] S. Liu and D. Sun, "Minimizing energy consumption of wheeled mobile robots via optimal motion planning," *Mechatronics, IEEE/ASME Transactions on*, vol. 19, no. 2, pp. 401–411, 2014.
- [8] H. Kim and B. K. Kim, "Online minimum-energy trajectory planning and control on a straight-line path for three-wheeled omnidirectional mobile robots," *Industrial Electronics, IEEE Transactions on*, vol. 61, no. 9, pp. 4771–4779, 2014.
- [9] A. Alessandretti, A. P. Aguiar, and C. N. Jones, "A model predictive control scheme with ultimate bound for economic optimization," in *American Control Conference (ACC)*, 2015.
- [10] A. Alessandretti, A. Aguiar, and C. N. Jones, "An economic model predictive control scheme with terminal penalty for continuous-time systems," in *IEEE Conference on Decision and Control and European Control Conference*, 2014.
- [11] R. Rajamani, *Vehicle dynamics and control*. Springer, 2011.
- [12] L. Guzzella and A. Sciarretta, *Vehicle propulsion systems*, vol. 1. Springer, 3 ed., 2013.
- [13] A. Alessandretti, A. P. Aguiar, and C. N. Jones, "Trajectory-tracking and path-following controllers for constrained underactuated vehicles using model predictive control," in *European Control Conference (ECC)*, pp. 1371–1376, Ieee, 2013.
- [14] S. Boyd and L. Vandenberghe, *Convex optimization*. Cambridge university press, 2004.
- [15] B. Houska, H. J. Ferreau, and M. Diehl, "Acado toolkit—an open-source framework for automatic control and dynamic optimization," *Optimal Control Applications and Methods*, vol. 32, no. 3, pp. 298–312, 2011.